ChemPubSoc Europe

DOI: 10.1002/cctc.201300212

CO Oxidation on Metal-Supported Ultrathin Oxide Films: What Makes Them Active?

Yulia Martynova, Shamil Shaikhutdinov,* and Hans-Joachim Freund[a]

Well-ordered, thin oxide films grown on single-crystal substrates have drawn some attention in recent years as suitable oxide supports for modeling highly dispersed metal catalysts at the atomic scale. A continuously growing body of experimental and theoretical results indicates that ultrathin oxide films, those below 1 nm in thickness, may exhibit interesting catalytic properties in their own right, which may not be observed on thicker films or respective single-crystal surfaces.[1] In particular, such films show a higher CO oxidation rate than "conventional" platinum group metal catalysts. For example, a FeO(111) monolayer (ML) film grown on Pt(111) is more active than thicker iron oxide films or clean Pt(111) if the reaction takes place at near-atmospheric pressures and low temperatures.[2] The activity of a 2 ML-thick MgO(100) film on Ag(100) has been predicted to be higher than that of Pt(111),[3] yet this awaits experimental proof. Although different reaction mechanisms for these two systems have been proposed, the common feature includes charge transfer from the oxide/metal interface to activate oxygen. In addition, this process is accompanied by an oxide lattice ("polaronic") distortion, which can readily be accommodated in a thin film, but is hardly possible in bulklike oxide films.[4] It is therefore anticipated that film thickness may affect the activity. In principle, the same picture holds true for "native" oxide films formed on metal surfaces under net oxidizing conditions. In essence, there is nothing that would change the underlying physical principles. At relatively high temperatures, even noble metals such as Pt, Pd, and Ag may possess a very thin, surface oxide overlayer. Perhaps the most explored and still controversially discussed example concerns CO oxidation over ruthenium catalysts.[5]

In fact, charge-transfer processes on oxide/metal interfaces were put forward a while ago, notably by Cabrera and Mott[6] who addressed the oxidation of metals. They assumed that the ability to transfer electrons to adsorbed oxygen to form a negatively charged species leads to an electric field that provides the driving force for the transport of metal ions from the metal/semiconductor interface to the surface to form additional layers of oxide. This process will stop as the layer becomes thicker. Certainly, for electron transfer by tunneling to be significant, the oxide film must be an insulator or semiconductor. However, the ability of even a "metallic" ultrathin oxide film, as it initially grows, to distort locally to accommodate charge that will concomitantly be stabilized by metallic screening may still be a decisive factor for its chemical reactivity.

In the early 1960s, there were attempts, most notably by Vol′kenstein[7] and Schwab[8] (see also a critical review by Slinkin and Fedorovskaya[9]), to develop the so-called "electron theory of catalysis" based, in essence, on the concept of Schottky barriers. However, at that time the preparation and atomic-scale characterization of thin oxide films was not feasible. Obviously, establishing direct relationships between the film structure and the reactivity requires controllable growth of well-ordered oxide films.

In this communication, we analyze the catalytic properties of ultrathin films of transition metal oxides by using the oxidation of CO at low temperatures and near-atmospheric pressures as a benchmark reaction. The systems include ultra-thin Fe oxide, Mn oxide, Zn oxide, and Ru oxide films. Structural characterization was performed by a number of "surface science" techniques such as a low-energy electron diffraction (LEED), Auger electron spectroscopy (AES), temperature-programmed desorption (TPD), and scanning tunneling microscopy (STM). We focus on finding key factors that govern the reaction in an attempt to rationalize structure–reactivity relationships for thin oxide films in oxidation reactions.

First, we recall the results of an FeO(111)/Pt(111) film that revealed a CO oxidation rate that was much higher than that of a Pt(111) support (Figure 1a). Under net oxidizing conditions, the film becomes enriched with oxygen and maintains long-range order. Density functional theory (DFT) calculations showed that oxygen in the gas phase interacts with the FeO bilayer film on Pt(111) by pulling an iron atom from the oxide/metal interface to the outermost layer. This lowers the work function locally and allows electron transfer to this oxygen atom accompanied by the formation of a transient O_2^- species, which then dissociates, and this results in a local O–Fe–O trilayer structure.[2a] Ultimately, such a trilayer with a compositional stoichiometry of FeO_2 (see schematic in Figure 1b) covers the whole Pt(111) support. The presence of a Moiré superstructure, as a result of a lattice mismatch of approximately 10% between FeO(111) and Pt(111), renders the real structure more complex.[10] Nonetheless, the trilayer can readily oxidize incoming CO to CO_2 by means of an Eley–Rideal mechanism to leave behind an oxygen vacancy in the film. Under net oxidizing conditions, the oxygen vacancy is replenished, and the trilayer film is sustained. In an O_2-lean atmosphere, however, the oxide film dewets to form small iron oxide particles on Pt(111), which determine (a relatively low) activity of the system most likely by reaction at the oxide/metal interface.[11] Therefore, to prevent film dewetting and hence deactivation, the reaction must be carried out at high ratios of O_2/CO. The chemical po-

[a] Y. Martynova, Dr. S. Shaikhutdinov, Prof. H.-J. Freund
Department of Chemical Physics
Fritz Haber Institute of the Max Planck Society
Faradayweg 4-6, Berlin 14195 (Germany)
Fax: (+49) 30-84134105
E-mail: shaikhutdinov@fhi-berlin.mpg.de

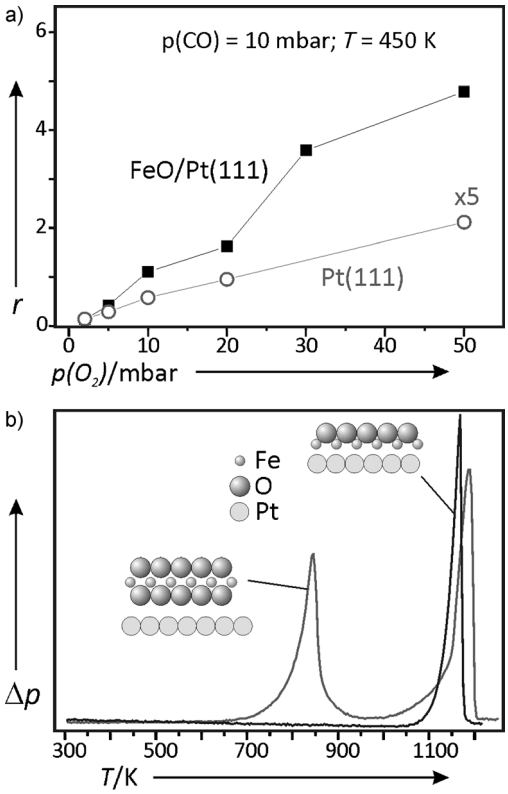

Figure 1. a) Reaction rates [a.u.] of Pt(111) and FeO(111)/Pt(111) at 450 K in the reaction mixture of 10 mbar CO and the indicated pressure of oxygen (He balance to 1 bar). b) Thermal desorption spectra of O_2 for a pristine FeO(111) film and for a film exposed to 20 mbar O_2 at 450 K. The FeO bilayer and O–Fe–O trilayer structures on Pt(111) are schematically shown.

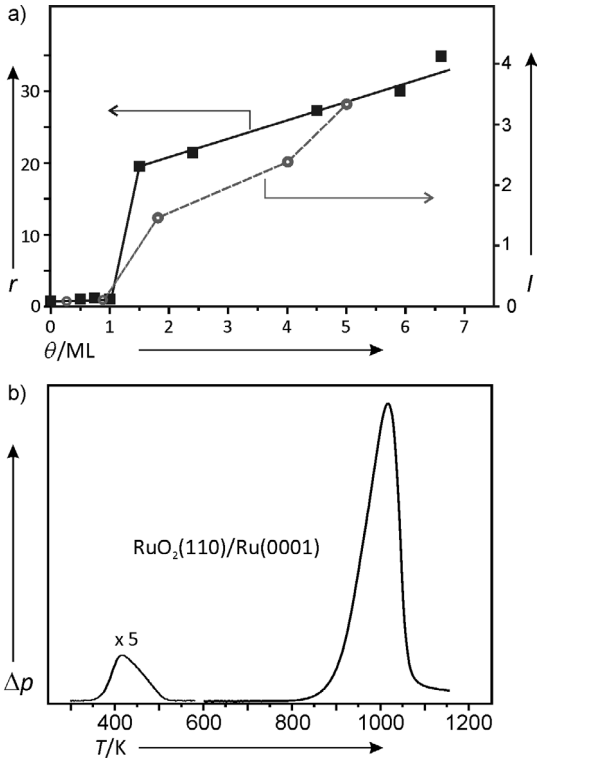

Figure 2. a) Turnover frequency [s^{-1}] as a function of oxygen coverage of an O-precovered Ru(0001) surface (oxygen coverage below 1 ML) and of Ru oxide films grown on Ru(0001) prior to the CO oxidation reaction, performed at 450 K in a mixture of 10 mbar CO and 50 mbar O_2 (He balance to 1 bar). The right axis shows the integral intensity of the 32 amu signals at approximately 420 K observed in the thermal desorption spectra of oxide films exposed to 20 mbar O_2 at 450 K. A typical spectrum is shown in b). The desorption signal at 420 K is assigned to the top O surface species on RuO_2(110), whereas desorption at $T > 900$ K is assigned to film decomposition ("lattice oxygen").

tential of oxygen (given by reaction pressure and temperature) controls the structural transformations of a film. Indeed, the LEED, AES, TPD, and STM results showed that the FeO_2-like structure is formed by exposure to elevated pressures of pure O_2. The thermal desorption spectra showed a strong desorption signal of oxygen at approximately 840 K, which is associated with the topmost oxygen atoms in a O–Fe–O trilayer, in addition to a peak at 1190 K, which is also observed for pristine bilayer films (Figure 1b). In agreement with this, DFT calculations showed that the O-vacancy formation energy in a trilayer film is much lower than that in a bilayer film.[2a]

To see whether a similar scenario could be applied to Ru catalysts in which a thin oxide overlayer is believed to be active, at least at low temperatures,[5a,12] we examined the reactivity of Ru oxide films on Ru(0001) by primarily focusing on its thickness dependence.[13] Note that the oxide films were prepared before the catalytic tests. As shown in Figure 2a, the oxidation of CO is initiated only in the presence of the oxidic phase, at which point the O coverage on Ru(0001) exceeds 1 ML. The reaction rate slightly increases with increasing amounts of oxygen incorporated into the film (measured by AES and TPD), that is, with increasing film thickness. A complementary TPD study of the films exposed to 20 mbar (1 mbar = 100 Pa) O_2 at 450 K (a typical spectrum is depicted in Figure 2b) revealed that the reaction rate basically follows the integral intensity of the oxygen desorption peak centered at approximately 420 K, previously assigned to terminal Ru=O species on RuO_2(110).[14] It is still unclear whether these species are directly involved in the reaction with co-adsorbed CO or if they only replenish the bridged oxygen species, albeit more strongly bound.[15] Nonetheless, it is clear that the oxide thickness is not crucial for the reaction. The reaction sets in as soon the oxidic phase builds up.

Comparison of the TPD spectra presented in Figures 1b and 2b reveals that surface oxygen species on RuO_2(110)/Ru(0001) films are much more weakly bound than on FeO_2/Pt(111) films (420 versus 840 K). In turn, the reaction rate on RuO_2(110)/Ru(0001) films is approximately three times higher than that on FeO_2/Pt(111) under the same reaction conditions (10 mbar CO, 50 mbar O_2, He balance to 1 bar, 450 K). Therefore, a comparative study of these two well-defined systems indicates that weakly bound oxygen is necessary for CO oxidation to occur at low temperatures.

The FeO_2 stoichiometry of the trilayer film on Pt(111) implies that the Fe atoms are in the formal 4+ oxidation state, which is very uncommon for iron oxides, and the DFT calculations indeed showed that the oxidation state of iron is close to 3+ owing to the presence of the Pt(111) substrate. However, there are transition metals that favor the 4+ state in the re-

quired MO_2 stoichiometry. Among those supported on Pt(111), ultrathin titania films seem to be the best characterized.[16] However, TiO_x films exhibit a very complex phase diagram, with several structures coexisting.

Recently, the preparation of well-ordered Mn oxide ultrathin films on Pt(111) was reported,[17] in which a MnO_2 film of a O–Mn–O trilayer structure was also considered.[18] Note that establishing direct relationships between the film thickness and the reactivity requires controllable growth of multilayer films in a layer-by-layer mode. This was impossible for FeO(111) films because of its polar instability, and thicker iron oxide films grew that exhibited a Fe_3O_4(111) spinel structure.[19] By surveying other potential systems suitable for this study, we found that ZnO(0001) films could, in principle, be grown layer-by-layer in the same manner as that observed on Pd(111).[20] Therefore, we examined CO oxidation on Mn oxide and Zn oxide thin films grown on Pt(111).

The "as-prepared" MnO monolayer films show a complex (19×1) superstructure, which was previously assigned to a non-polar, [001]-oriented MnO layer on Pt(111) exhibiting uniaxial reconstruction.[17a] At high pressures of O_2 (in the mbar range), the MnO films showed oxygen enrichment close to a MnO_2 stoichiometry, as judged by AES. The films do not dewet, although long-range ordering is strongly suppressed.[21] Additional O_2 desorption peaks at 950 and 1060 K were observed in the TPD spectra of these "O-rich" films, as shown in Figure 3a. It seems plausible, yet not proven, that the film reconstructs, at least partially, into the O–Mn–O trilayer structure.

Well-ordered thin ZnO(0001) films can, indeed, be grown on Pt(111) in a layer-by-layer mode.[22] Previous studies on Ag(111) and Pd(111) supports[20,23] revealed that the thinnest ZnO films resemble the co-planar sheets in the hexagonal boron nitride (or graphite) structure, and transition to the bulk wurtzite structure occurs for thicker (≈4–5 ML) films. Our STM results showed that at high oxygen pressures, a ZnO monolayer film on Pt(111) is not stable and transforms into two monolayer-thick islands. Therefore, precautions had to be taken for preparing the films uniformly covering a whole Pt(111) support. Irrespective of the film thickness, the TPD spectra of closed films exposed to 20 mbar O_2 showed only one desorption peak at approximately 1020 K (Figure 3a). Recent DFT calculations showed that oxygen does not adsorb onto an O-terminated ZnO(0001) surface, but very strongly onto a Zn-terminated ZnO(000-1) surface.[24] Therefore, it is most likely that exposure to high O_2 pressures either causes interlayer relaxations, favoring an O-terminated surface, or creates the O-ZnO(0001) surface. Accordingly, these films do not contain oxygen surface species other than those belonging to the ZnO crystal structure. (Although the presence of additional oxygen atoms directly bonded to a metal support at the interface cannot be ruled out,[25] those are hardly accessible for CO molecules.)

Finally, we made a few attempts to grow well-ordered Ru oxide films on Pt(111) to compare such films with "native" oxide films formed on Ru(0001), which exhibit a very high CO oxidation rate. Unfortunately, only amorphous RuO_2 films could be prepared. It turned out, however, that the films grown on Pt(111) to a thickness similar to that on Ru(0001) do not show an O_2 desorption signal at 420 K, which is observed on RuO_2(110)/Ru(0001), but instead a broad shoulder centered at approximately 820 K (Figure 3a).

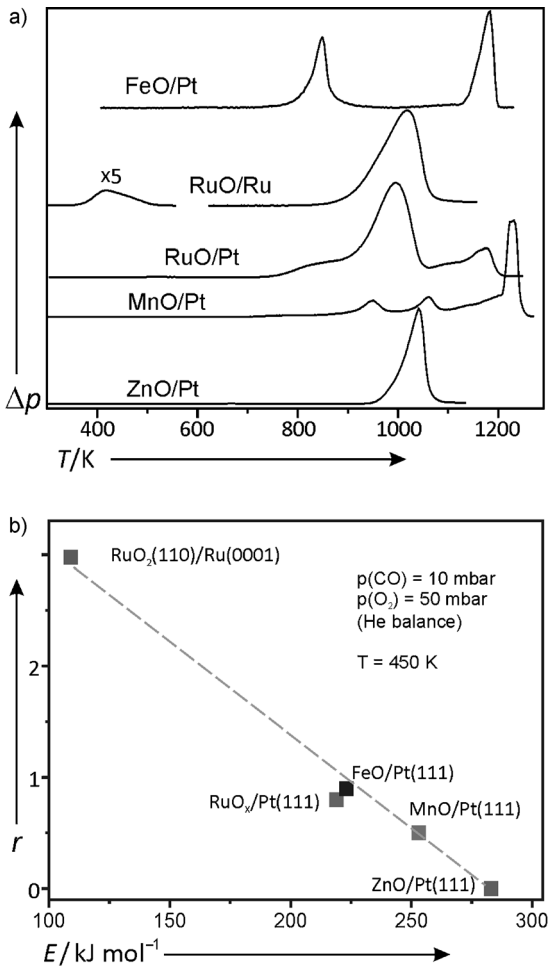

Figure 3. a) Thermal desorption spectra of O_2 (32 amu) for a series of ultrathin oxide films, all exposed to 20 mbar O_2 at 450 K. The heating rate was 5 K s^{-1}. b) Initial CO_2 production rate (at zero conversion) measured at 450 K in a mixture of 10 mbar CO and 50 mbar O_2 (He balance to 1 bar) as a function of the desorption energy of the most weakly bound oxygen obtained from the TPD spectra shown in a).

We are now in the position to link the state of oxygen to the activity of the ultrathin films in the low-temperature oxidation of CO. Figure 3a collects the 32 amu signals in the TPD spectra of the various films, all treated with 20 mbar O_2 at 450 K for 10 min to mimic net oxidizing conditions used for reactivity measurements. It is clear that RuO_2(110) films on Ru(0001) possess the most weakly bound oxygen amongst these films, whereas the ZnO films only show a peak associated with lattice oxygen. Figure 3b displays the CO_2 production rate in the reaction mixture of 10 mbar CO and 50 mbar O_2 (He balance to 1 bar) at 450 K as a function of the desorption energy of the most weakly bound oxygen species in the respective films. The oxygen desorption energies were calculated from the TPD spectra by using the Redhead approximation with the conventionally used prefactor 10^{13} s^{-1}.[26] The reaction rates were all measured within the first 5–10 min of the

steady-state reaction so that catalyst deactivation, if any, could be neglected.

Figure 3b provides compelling evidence that oxygen binding energy in the films play a decisive role in the CO oxidation reaction under these conditions. The lower the energy of weakly bound surface oxygen species, the higher the reaction rate. Such a relationship is also reflected in the apparent activation energies, which are found to be approximately 58 and 113 kJ mol^{-1} for the RuO_2(110)/Ru(0001) and FeO(111)/Pt(111) systems, respectively.[2b,13] The RuO_x films on Ru(0001) show much higher activity than those on Pt(111), and this suggests that the CO oxidation reaction on Ru oxides is structure sensitive in a way that the RuO_2(110) phase formed on Ru(0001), but not on Pt(111), provides weakly bound oxygen species to react with CO.

The CO oxidation reaction on metal surfaces is commonly considered within the Langmuir–Hinshelwood (L–H) mechanism, in which the reaction takes place between chemisorbed CO and O. For oxide surfaces, however, the Eley–Rideal (E–R) mechanism, in which the reaction occurs between gas-phase CO and chemisorbed O, seems to be operative as well, albeit case sensitive. Indeed, previous DFT studies indicated that the L–H mechanism dominates on RuO_2(110),[27] whereas the E–R mechanism determines the reactivity of O-terminated FeO_2(111)/Pt(111).[2a] Another scenario would occur if the reaction were triggered by the E–R mechanism to open Lewis acid sites (i.e., metal cations) on the surface for CO, which then adsorbs and reacts with the surrounding oxygen species so that the reaction would be sustained by the L–H mechanism {see similar considerations for an O(1×1)-Ru(0001) surface[28]}. If applied to a FeO/Pt system, the latter scenario would suggest that CO first reacts with oxygen in the top layer of the O–Fe–O trilayer. This would thus create oxygen vacancies, which either may adsorb CO on the exposed Fe cations or would be replenished by the reaction with ambient O_2. Both pathways can, in principle, be affected by the lattice flexibility of the film and most likely depend on the CO/O_2 ratio in the gas mixture, which also governs film dewetting.[2b]

It is well known that CO rather weakly binds to oxide surfaces, particularly to O-terminated surfaces. Therefore, increasing the binding energy of CO would enhance the activity. Indeed, the reaction rate on a ZnO film that only partially covers a Pt(111) surface increases by a factor of 5–10 relative to the reaction rate of a closed film.[22] Obviously, one of the reasons for the rate enhancement is the much stronger adsorption of CO on Pt than on ZnO.[29] In turn, this increases the residence time of CO on the surface in the vicinity of the ZnO islands and hence increases the probability to react with an oxygen at the island rim. The results nicely fit the model of overlapping states,[30] which states that desorption profiles of two reacting entities must overlap for the reaction to occur. Therefore, shifting the oxygen desorption temperature to lower values will enhance reactivity, as indeed observed in Figure 3b.

Notably, there were attempts in the past to link metal–oxygen bond energy and activity in the oxidation of CO on metals.[31] When measured at low pressures ($\approx 10^{-7}$ mbar) at 520 K, the activity followed a row: Pt, Pd, Rh > Ir ≫ Ru, Ni. The low activity of Ru and Ni foils was attributed to a very strong adsorption of oxygen. Although further studies revealed that the reaction is much more complex at elevated pressures as a result of the possible formation of oxide overlayers on metal surfaces,[32] such an inverse relationship is characteristic of a rate-limiting reaction between surface O and CO. However, a comparative study of CO + O_2 and CO + NO reactions on FeO films indicated that the rate-limiting step is likely the replenishment of the oxygen vacancies.[33] In this respect, isotopic experiments on RuO_2(110) films,[15] albeit performed at low pressures, indicated that weakly bound oxygen is used for oxygen replenishment rather than being directly involved in the reaction.

Certainly, there may be several types of oxygen species present on oxide surfaces that complicate the reaction mechanism even further. Nonetheless, the presented analysis shows that oxygen binding energy can serve as a good descriptor for this reaction on thin oxide films.

Experimental Section

The experiments were performed in an ultrahigh vacuum chamber (base pressure 2×10^{-10} mbar) equipped with LEED, AES, and a mass spectrometer for TPD measurements.[2b] The chamber houses a gold-plated reaction cell for reactivity studies at atmospheric pressures by using a gas chromatograph (GC). The double-side polished crystal [Pt(111) or Ru(0001)] was spot-welded to thin Ta wires for resistive heating. The sample temperature was measured by a Type K thermocouple spot-welded to the edge of the crystal. The preparation of the oxide films is described in detail elsewhere[13,17b,19,22] and includes metal deposition onto a metal substrate and subsequent oxidation at approximately 10^{-6} mbar O_2 at elevated temperatures. The reaction gas mixture, balanced with He to 1 bar, was dosed at room temperature and circulated by using a membrane pump ($\approx$3 mL min^{-1}). Then the sample was heated to 450 K, and the reaction was monitored by GC.

Acknowledgements

The work was supported by Fonds der Chemischen Industrie, Deutsche Forschungsgemeinschaft, and Cluster of Excellence "UniCat".We also acknowledge the support from the COST Action CM1104 "Reducible oxide chemistry, structure and functions"

Keywords: carbon monoxide · oxidation · model catalysts · thin films · oxide films

[1] a) L. Giordano, G. Pacchioni, *Acc. Chem. Res.* **2011**, *44*, 1244–1252; b) H.-J. Freund, G. Pacchioni, *Chem. Soc. Rev.* **2008**, *37*, 2224–2242; c) F. P. Netzer, F. Allegretti, S. Surnev, *J. Vac. Sci. Technol. B* **2010**, *28*, 1–16; d) S. Shaikhutdinov, H.-J. Freund, *Annu. Rev. Phys. Chem.* **2012**, *63*, 619–633.
[2] a) Y.-N. Sun, L. Giordano, J. Goniakowski, M. Lewandowski, Z.-H. Qin, C. Noguera, S. Shaikhutdinov, G. Pacchioni, H.-J. Freund, *Angew. Chem.* **2010**, *122*, 4520–4523; *Angew. Chem. Int. Ed.* **2010**, *49*, 4418–4421; b) Y. N. Sun, Z. H. Qin, M. Lewandowski, E. Carrasco, M. Sterrer, S. Shaikhutdinov, H. J. Freund, *J. Catal.* **2009**, *266*, 359–368.
[3] A. Hellman, S. Klacar, H. Grönbeck, *J. Am. Chem. Soc.* **2009**, *131*, 16636–16637.

[4] A. Gonchar, T. Risse, H.-J. Freund, L. Giordano, C. Di Valentin, G. Pacchioni, *Angew. Chem.* **2011**, *123*, 2684 – 2687; *Angew. Chem. Int. Ed.* **2011**, *50*, 2635 – 2638.
[5] a) H. Over, *Chem. Rev.* **2012**, *112*, 3356 – 3426; b) F. Gao, Y. Wang, Y. Cai, D. W. Goodman, *Surf. Sci.* **2009**, *603*, 1126 – 1134; c) H. Over, Y. D. Kim, A. P. Seitsonen, S. Wendt, E. Lundgren, M. Schmid, P. Varga, A. Morgante, G. Ertl, *Science* **2000**, *287*, 1474 – 1476.
[6] N. Cabrera, N. F. Mott, *Rep. Prog. Phys.* **1949**, *12*, 163.
[7] F. F. Vol'kenshtein, *Russ. Chem. Rev.* **1966**, *35*, 537.
[8] G.-M. Schwab, *Adv. Catal.* **1979**, *27*, 1 – 22.
[9] A. A. Slinkin, E. A. Fedorovskaya, *Russ. Chem. Rev.* **1971**, *40*, 860.
[10] L. Giordano, M. Lewandowski, I. M. N. Groot, Y. N. Sun, J. Goniakowski, C. Noguera, S. Shaikhutdinov, G. Pacchioni, H. J. Freund, *J. Phys. Chem. C* **2010**, *114*, 21504 – 21509.
[11] Y.-N. Sun, Z.-H. Qin, M. Lewandowski, S. Kaya, S. Shaikhutdinov, H.-J. Freund, *Catal. Lett.* **2008**, *126*, 31 – 35.
[12] F. Gao, D. W. Goodman, *Phys. Chem. Chem. Phys.* **2012**, *14*, 6688 – 6697.
[13] Y. Martynova, B. Yang, X. Yu, J. A. Boscoboinik, S. Shaikhutdinov, H. J. Freund, *Catal. Lett.* **2012**, *142*, 657 – 663.
[14] Y. D. Kim, A. P. Seitsonen, S. Wendt, J. Wang, C. Fan, K. Jacobi, H. Over, G. Ertl, *J. Phys. Chem. B* **2001**, *105*, 3752 – 3758.
[15] S. Wendt, M. Knapp, H. Over, *J. Am. Chem. Soc.* **2004**, *126*, 1537 – 1541.
[16] G. Barcaro, S. Agnoli, F. Sedona, G. A. Rizzi, A. Fortunelli, G. Granozzi, *J. Phys. Chem. C* **2009**, *113*, 5721 – 5729.
[17] a) C. Hagendorf, S. Sachert, B. Bochmann, K. Kostov, W. Widdra, *Phys. Rev. B* **2008**, *77*, 075406; b) S. Sachert, S. Polzin, K. Kostov, W. Widdra, *Phys. Rev. B* **2010**, *81*, 195424.
[18] S. Sachert, Martin-Luther-Universität Halle-Wittenberg (Halle), **2008**.
[19] W. Weiss, M. Ritter, *Phys. Rev. B* **1999**, *59*, 5201 – 5213.
[20] G. Weirum, G. Barcaro, A. Fortunelli, F. Weber, R. Schennach, S. Surnev, F. P. Netzer, *J. Phys. Chem. C* **2010**, *114*, 15432 – 15439.
[21] Y. Martynova, M. Soldemo, J. Weissenrieder, S. Shaikhutdinov, H. J. Freund, unpublished results.
[22] Y. Martynova, B. H. Liu, M. E. McBriarty, I. M. N. Groot, M. J. Bedzyk, S. Shaikhutdinov, H. J. Freund, *J. Catal.* **2013**, *301*, 227 – 232.
[23] C. Tusche, H. L. Meyerheim, J. Kirschner, *Phys. Rev. Lett.* **2007**, *99*, 026102.
[24] J. Sołtys, J. Piechota, S. Krukowski, *DPG Meeting*, *Berlin* **2012**. ##http://www.dpg-verhandlungen.de/year/2012/conference/berlin/part/o/session/58/contribution/54.
[25] B. Bienek, Y. Xu, P. Rinke, M. Scheffler, private communication.
[26] P. A. Redhead, *Vacuum* **1962**, *12*, 203 – 211.
[27] K. Reuter, M. Scheffler, *Phys. Rev. B* **2006**, *73*, 045433.
[28] C. Stampfl, M. Scheffler, *Phys. Rev. Lett.* **1997**, *78*, 1500 – 1503.
[29] D. Sun, X.-K. Gu, R. Ouyang, H.-Y. Su, Q. Fu, X. Bao, W.-X. Li, *J. Phys. Chem. C* **2012**, *116*, 7491 – 7498.
[30] A. M. Doyle, S. K. Shaikhutdinov, H. J. Freund, *J. Catal.* **2004**, *223*, 444 – 453.
[31] V. I. Savchenko, *Russ. Chem. Rev.* **1986**, *55*, 222.
[32] a) Y. B. He, A. Stierle, W. X. Li, A. Farkas, N. Kasper, H. Over, *J. Phys. Chem. C* **2008**, *112*, 11946 – 11953; b) E. Lundgren, A. Mikkelsen, J. N. Andersen, G. Kresse, M. Schmid, P. Varga, *J. Phys. Condens. Matter* **2006**, *18*, R481; c) J. Gustafson, A. Mikkelsen, M. Borg, E. Lundgren, L. Köhler, G. Kresse, M. Schmid, P. Varga, J. Yuhara, X. Torrelles, C. Quirós, J. N. Andersen, *Phys. Rev. Lett.* **2004**, *92*, 126102; d) J. Gustafson, R. Westerström, A. Mikkelsen, X. Torrelles, O. Balmes, N. Bovet, J. N. Andersen, C. J. Baddeley, E. Lundgren, *Phys. Rev. B* **2008**, *78*, 045423.
[33] Y. Lei, M. Lewandowski, Y.-N. Sun, Y. Fujimori, Y. Martynova, I. M. N. Groot, R. J. Meyer, L. Giordano, G. Pacchioni, J. Goniakowski, C. Noguera, S. Shaikhutdinov, H.-J. Freund, *ChemCatChem* **2011**, *3*, 671 – 674.

Received: March 20, 2013
Published online on May 31, 2013